

Fermi-LAT Observations of Gamma-Ray Emission Toward the the Outer Halo of M31

To appear in
The Astrophysical Journal

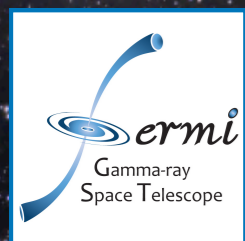
with **Simona Murgia,**
Sheldon Campbell, and
Igor Moskalenko

Chris Karwin
University of California, Irvine

36th ICRC
July, 26 2019

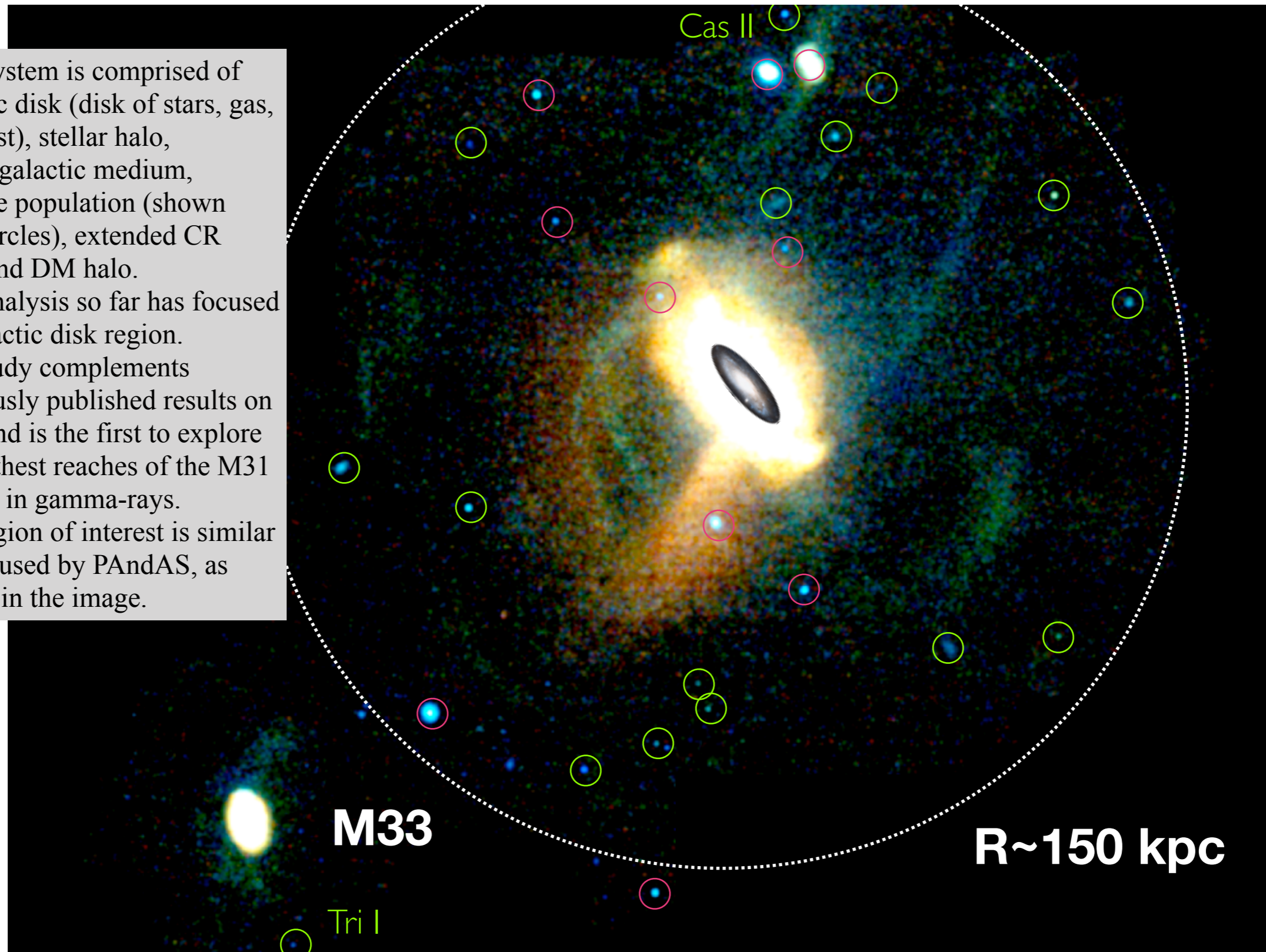
arXiv:
1903.10533

Image Credit: Miguel Claro



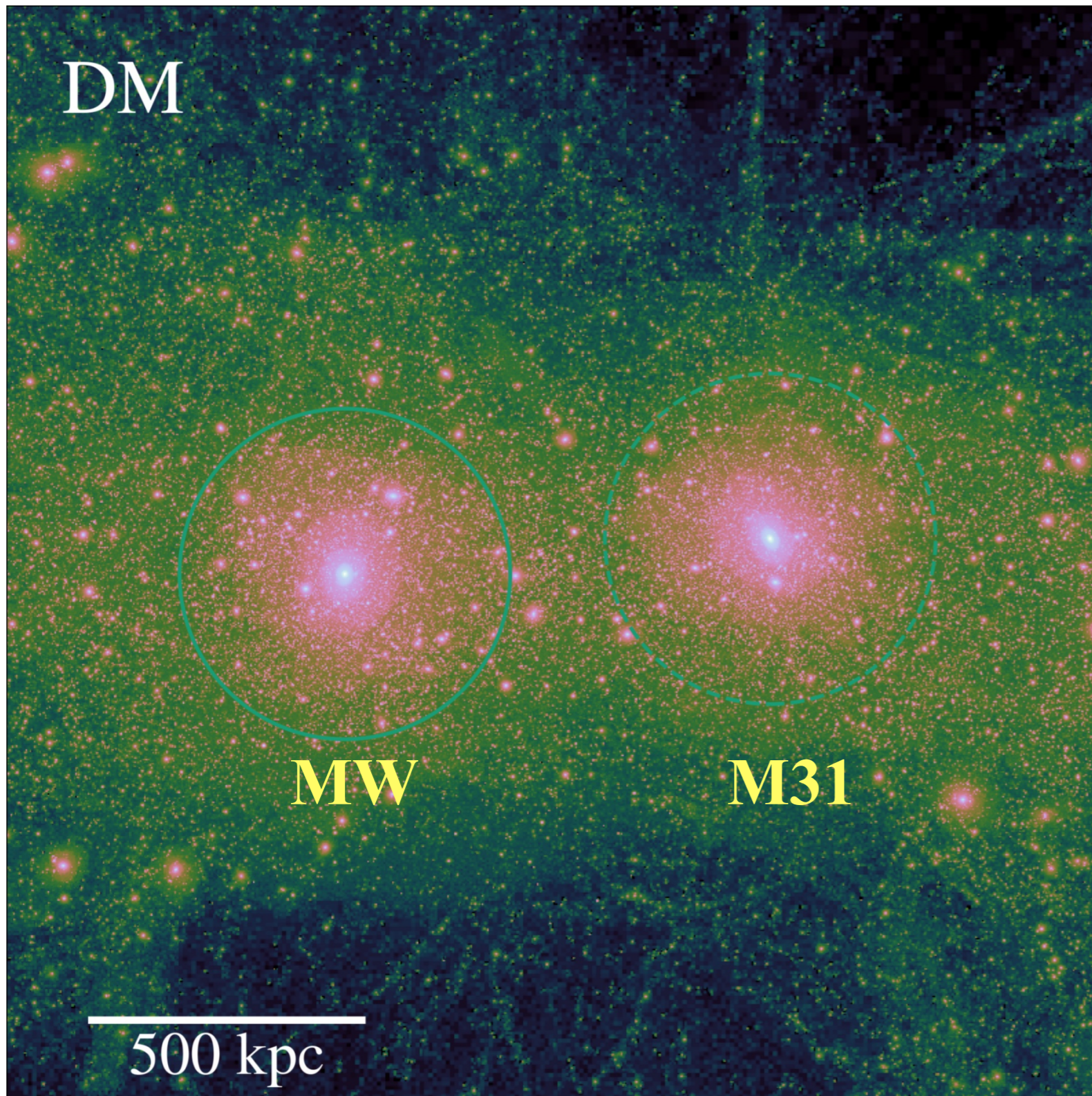
The M31 System

- M31 system is comprised of galactic disk (disk of stars, gas, and dust), stellar halo, circumgalactic medium, satellite population (shown with circles), extended CR halo, and DM halo.
- LAT analysis so far has focused on galactic disk region.
- Our study complements previously published results on M31 and is the first to explore the farthest reaches of the M31 system in gamma-rays.
- Our region of interest is similar to that used by PAndAS, as shown in the image.



credit: PAndAS, Martin et al. 2013

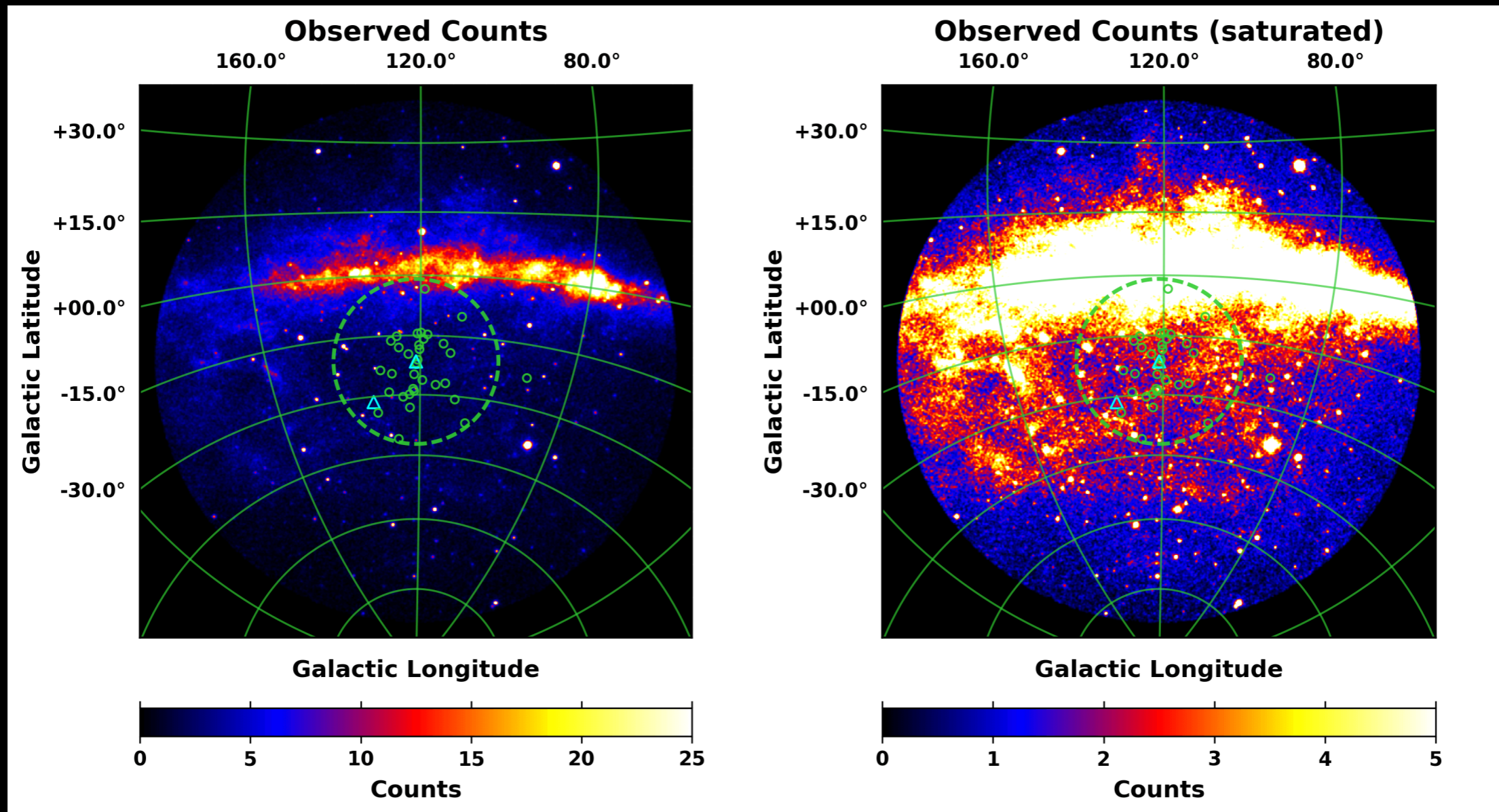
The M31 System (Dark Matter)



- M31 harbors a massive dark matter (DM) halo which may span up to ~ 600 kpc across and comprises $\sim 90\%$ of the galaxy's total mass.
- This halo size translates into a large diameter of 42° on the sky for an M31-Milky Way (MW) distance of 785 kpc, but its presumably low surface brightness makes it challenging to detect with gamma-ray telescopes.
- The entire M31 DM halo is seen from the outside, so we see the extended integral signal. For the MW we see through the halo, so it can be easily confused with diffuse components.
- Line of sight ostensibly includes:
M31 DM halo + secondary M31 emission + local DM filament between M31 and MW + MW DM halo.

credit: Garrison-Kimmel et al. 2018

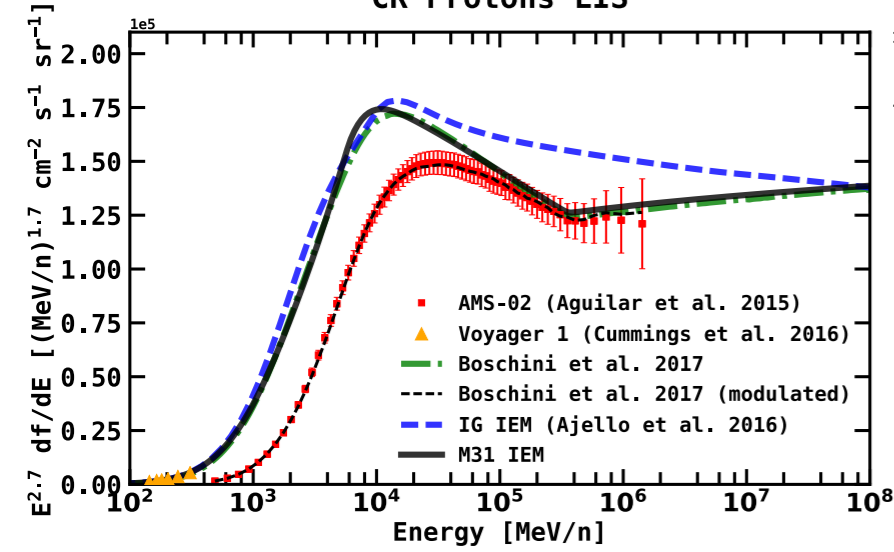
Fermi-LAT Observations



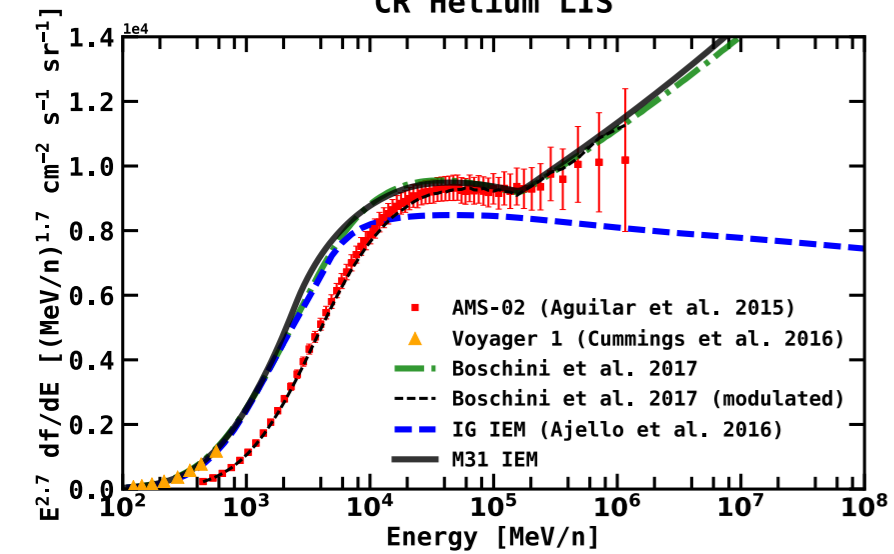
- Data: 7.6 years (2008-08-04 to 2016-03-16)
- Full ROI is a 60° radius centered at the position of M31
- Energy range: 1-100 GeV in 20 bins logarithmically spaced
- left: full count range. right: saturated counts, emphasizing lower counts at high latitudes.
- Dashed green circle (21° in radius) corresponds to a 300 kpc projected radius, for an M31-MW distance of 785 kpc
- M31 and M33 are shown with cyan triangles, and the rest of M31's dwarf galaxy population are shown with small green circles.
- **The primary purpose of the overlay is to provide a qualitative representation of M31's outer halo and to show its relationship to the MW disk.**

GALPROP Parameters

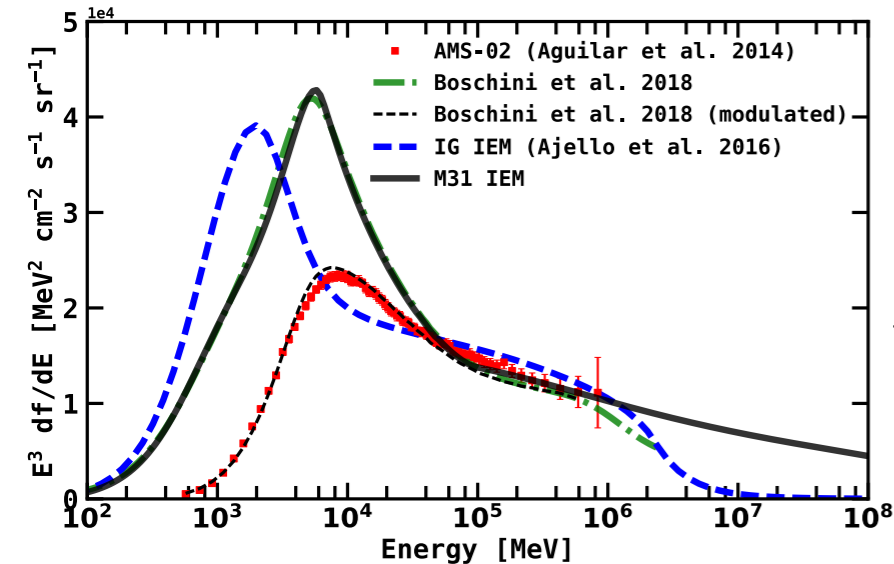
CR Protons LIS



CR Helium LIS



CR Electrons + Positrons LIS



| Parameter | M31 IEM | IG IEM |
|---|-------------|-----------|
| ^a z [kpc] | 4 | 6 |
| ^a r [kpc] | 20 | 30 |
| ^b a | 1.5 | 1.64 |
| ^b b | 3.5 | 4.01 |
| ^b r_1 | 0.0 | 0.55 |
| ^c D_0 [10^{28} cm ² s ⁻¹] | 4.3 | 7.87 |
| ^c δ | 0.395 | 0.33 |
| ^c η | 0.91 | 1.0 |
| ^c Alfvén speed, v_A [km s ⁻¹] | 28.6 | 34.8 |
| ^d $v_{\text{conv},0}$ [km s ⁻¹] | 12.4 | ... |
| ^d dv_{conv}/dz [km s ⁻¹ kpc ⁻¹] | 10.2 | ... |
| ^e $R_{p,0}$ [GV] | 7 | 11.6 |
| ^e $R_{p,1}$ [GV] | 360 | ... |
| ^e $\gamma_{p,0}$ | 1.69 | 1.90 |
| ^e $\gamma_{p,1}$ | 2.44 | 2.39 |
| ^e $\gamma_{p,2}$ | 2.295 | ... |
| ^e $R_{\text{He},0}$ [GV] | 7 | ... |
| ^e $R_{\text{He},1}$ [GV] | 330 | ... |
| ^e $\gamma_{\text{He},0}$ | 1.71 | ... |
| ^e $\gamma_{\text{He},1}$ | 2.38 | ... |
| ^e $\gamma_{\text{He},2}$ | 2.21 | ... |
| ^e $R_{e,0}$ [GV] | 0.19 | ... |
| ^e $R_{e,1}$ [GV] | 6 | 2.18 |
| ^e $R_{e,2}$ [GV] | 95 | 2171.7 |
| ^e $\gamma_{e,0}$ | 2.57 | ... |
| ^e $\gamma_{e,1}$ | 1.40 | 1.6 |
| ^e $\gamma_{e,2}$ | 2.80 | 2.43 |
| ^e $\gamma_{e,3}$ | 2.40 | 4.0 |
| ^f J_p [10^{-9} cm ⁻² s ⁻¹ sr ⁻¹ MeV ⁻¹] | 4.63 | 4.0 |
| ^f J_e [10^{-11} cm ⁻² s ⁻¹ sr ⁻¹ MeV ⁻¹] | 1.44 | 0.011 |
| ^g A5 [kpc] | 8–10 | 8–10 |
| ^g A6 [kpc] | 10–11.5 | 10–50 |
| ^g A7 [kpc] | 11.5–16.5 | ... |
| ^g A8 [kpc] | 16.5–50 | ... |
| ^h IC Formalism | Anisotropic | Isotropic |

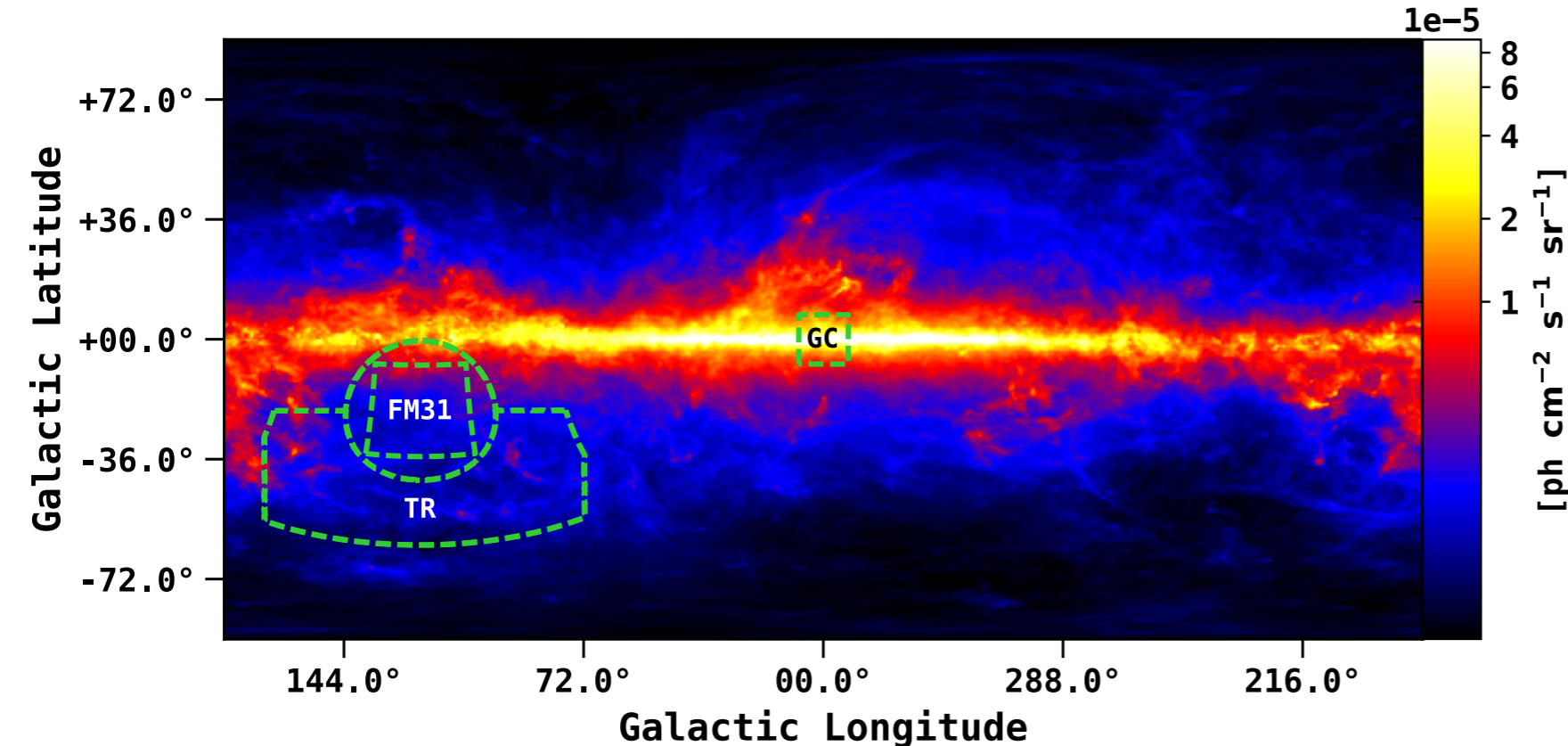
$$\rho(r) = \left(\frac{r + r_1}{r_\odot + r_1} \right)^a \times \exp \left(-b \times \frac{r - r_\odot}{r_\odot + r_1} \right)$$

$$q(R) \propto (R/R_0)^{-\gamma_0} \prod_{i=0}^2 \left[1 + (R/R_i)^{\frac{\gamma_i - \gamma_{i+1}}{s_i}} \right]^{s_i}$$

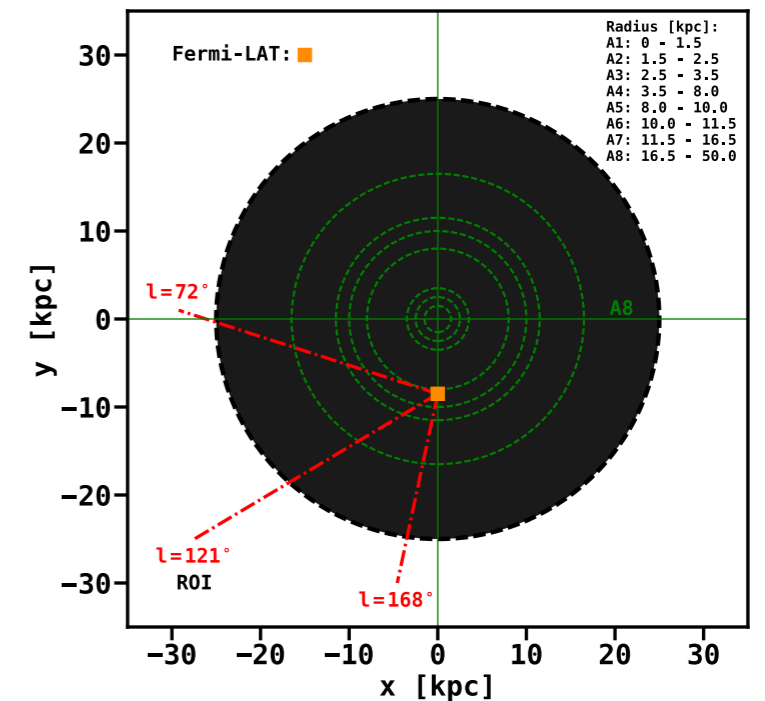
- GALPROP-based (v56) combined diffusion-convection-reacceleration model with a uniform spatial diffusion coefficient and a single power law index over the entire rigidity range.
- Injection and diffusion parameters are derived from local CR measurements, including AMS-02 and Voyager 1.
- Use the GALPROP parameters from Boschini et al. 2017,2018, which employ GALPROP and HelMod.
- CR source density based on the distribution of pulsars.
- IG IEM from Ajello et al. 2016 used as a reference model in our study of the systematics for the M31 field.

Interstellar Emission Model

Total Interstellar Emission Model



Milky Way Galaxy (overhead view)



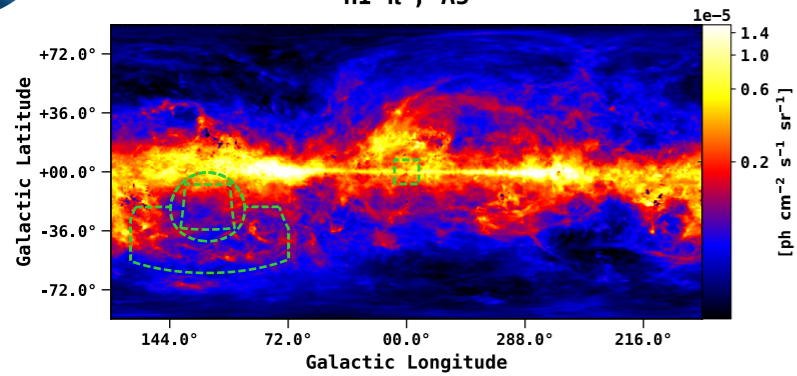
Gas is placed at Galactocentric radii based on Doppler shifted emission and Galactic rotational models (Ackerman et al 2012):

$$v_{\text{LSR}} = R_{\odot} \left(\frac{V(R)}{R} - \frac{V_{\odot}}{R_{\odot}} \right) \sin(l) \cos(b).$$

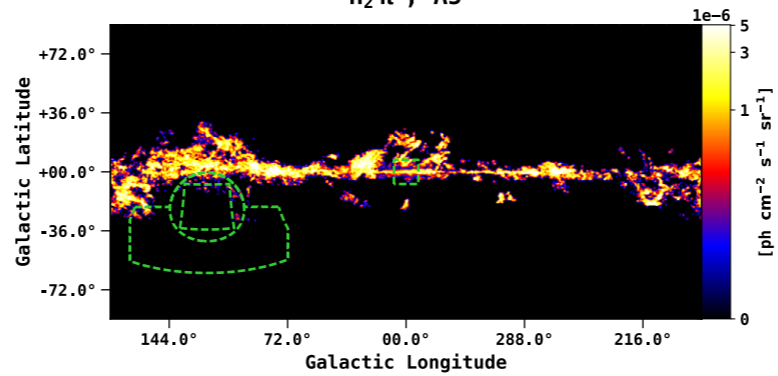
- Total IEM for the MW integrated between 1-100 GeV.
- The color corresponds to the intensity and is shown in log scale. The intensity level corresponds to the initial GALPROP output, before tuning to the gamma-ray data.
- IEM has contributions from pi-0 decay, (anisotropic) IC emission, and Bremsstrahlung emission (see next slide).
- IEM is defined in Galactocentric annuli (A1-A8), but only A5-A8 contribute to the foreground emission towards M31.
- The green dashed circle corresponds to M31's virial radius. Our primary field of interest, FM31, lies within the virial radius, and we use the region outside (and below latitudes of -21.5°) as a tuning region (TR).
- For reference we also show the GC region, which corresponds to a $15^\circ \times 15^\circ$ square centered at the GC.

Interstellar Emission Model

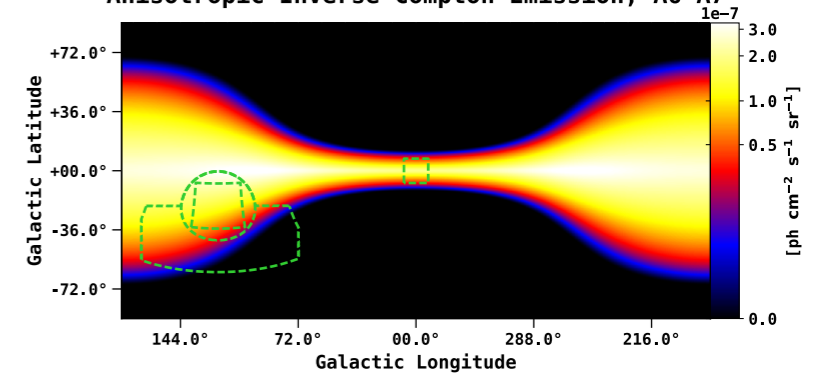
HI π^0 , A5



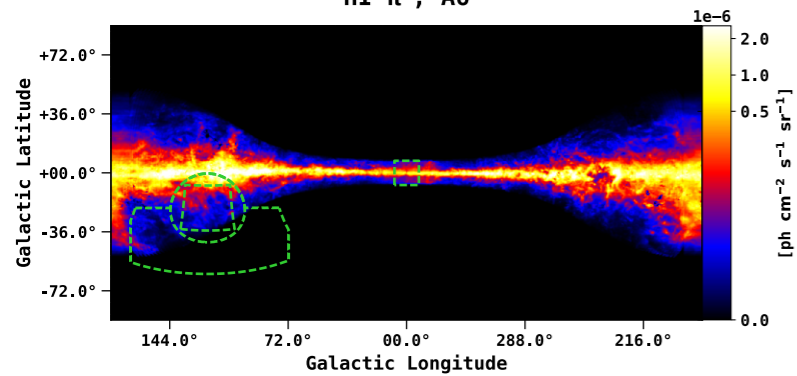
H₂ π^0 , A5



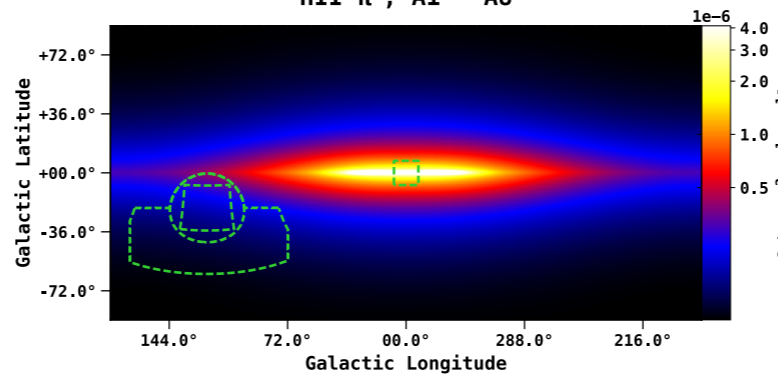
Anisotropic Inverse Compton Emission, A6-A7



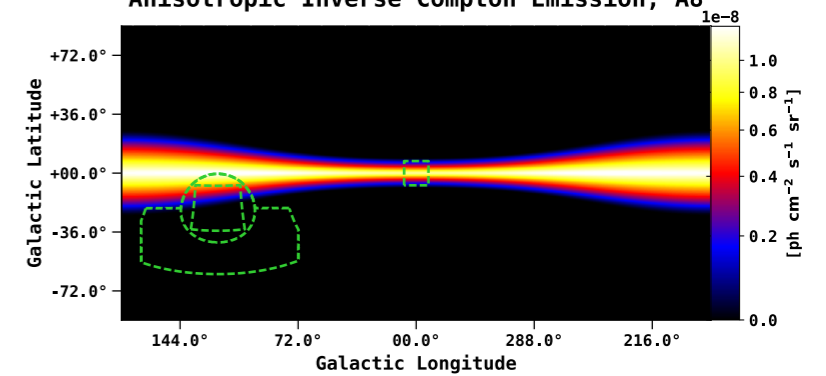
HI π^0 , A6



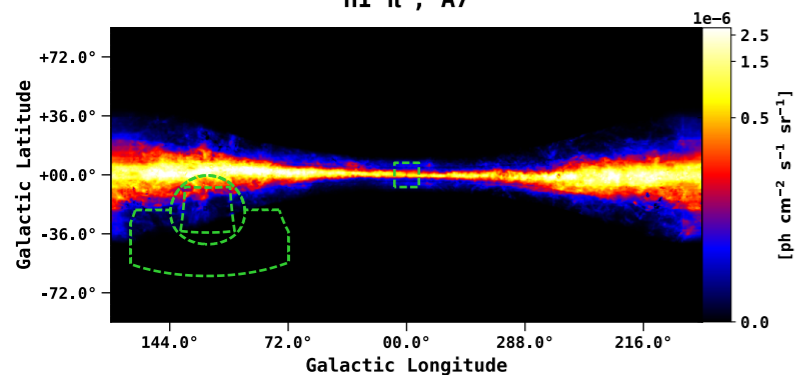
HII π^0 , A1 - A8



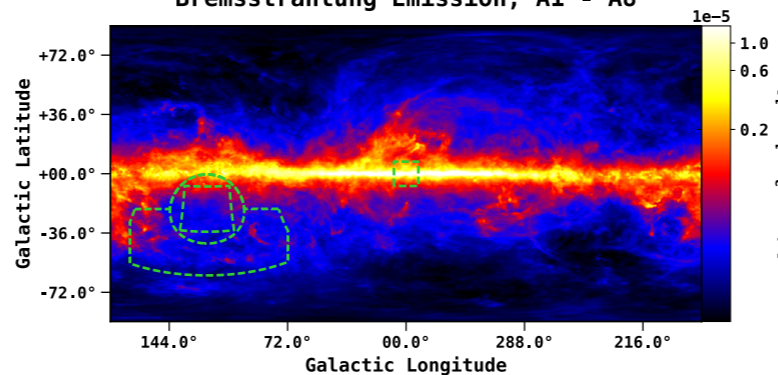
Anisotropic Inverse Compton Emission, A8



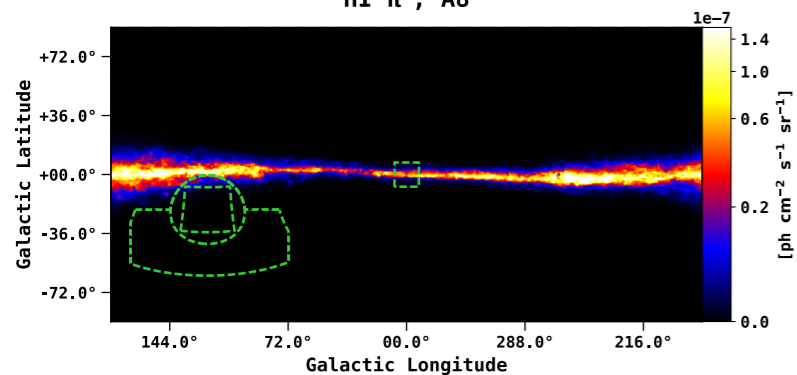
HI π^0 , A7



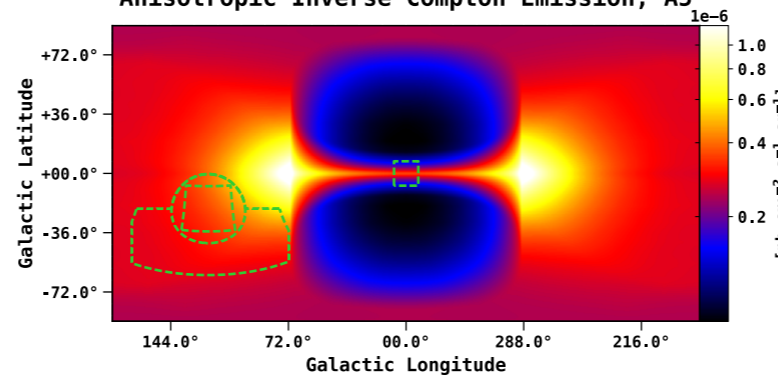
Bremsstrahlung Emission, A1 - A8



HI π^0 , A8



Anisotropic Inverse Compton Emission, A5



- FM31 has a significant contribution from emission related to H I gas, but there is very little contribution for H₂ gas.
- H I map GALPROP employs is based on LAB +GASS data, which for our ROI corresponds to LAB data only.
- A uniform spin temperature of 150 K is assumed.
- Our model also accounts for the dark neutral medium.
- The distribution of He in the interstellar gas is assumed to follow that of hydrogen, with a He/H ratio of 0.11 by number.
- Anisotropic formalism used for IC calculation.
- H I A5 and IC A5 are the dominant contributions in FM31 below ~ 5 GeV.
- IC A8 has minor contribution towards top of the field.

Isotropic Component

Isotropic Calculation for IG IEM, corresponding to the gray band in the bigger figure.

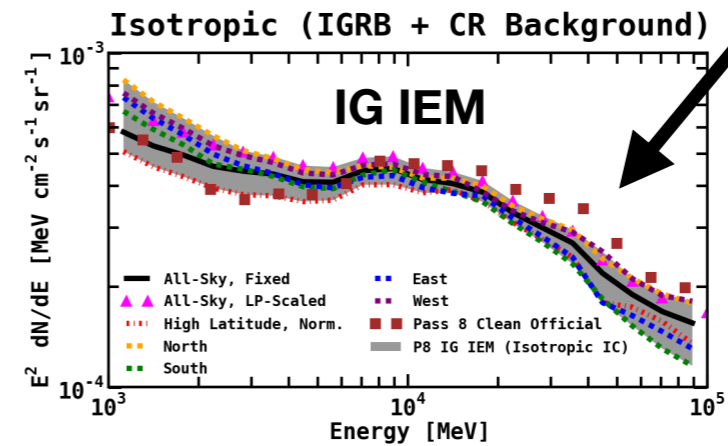
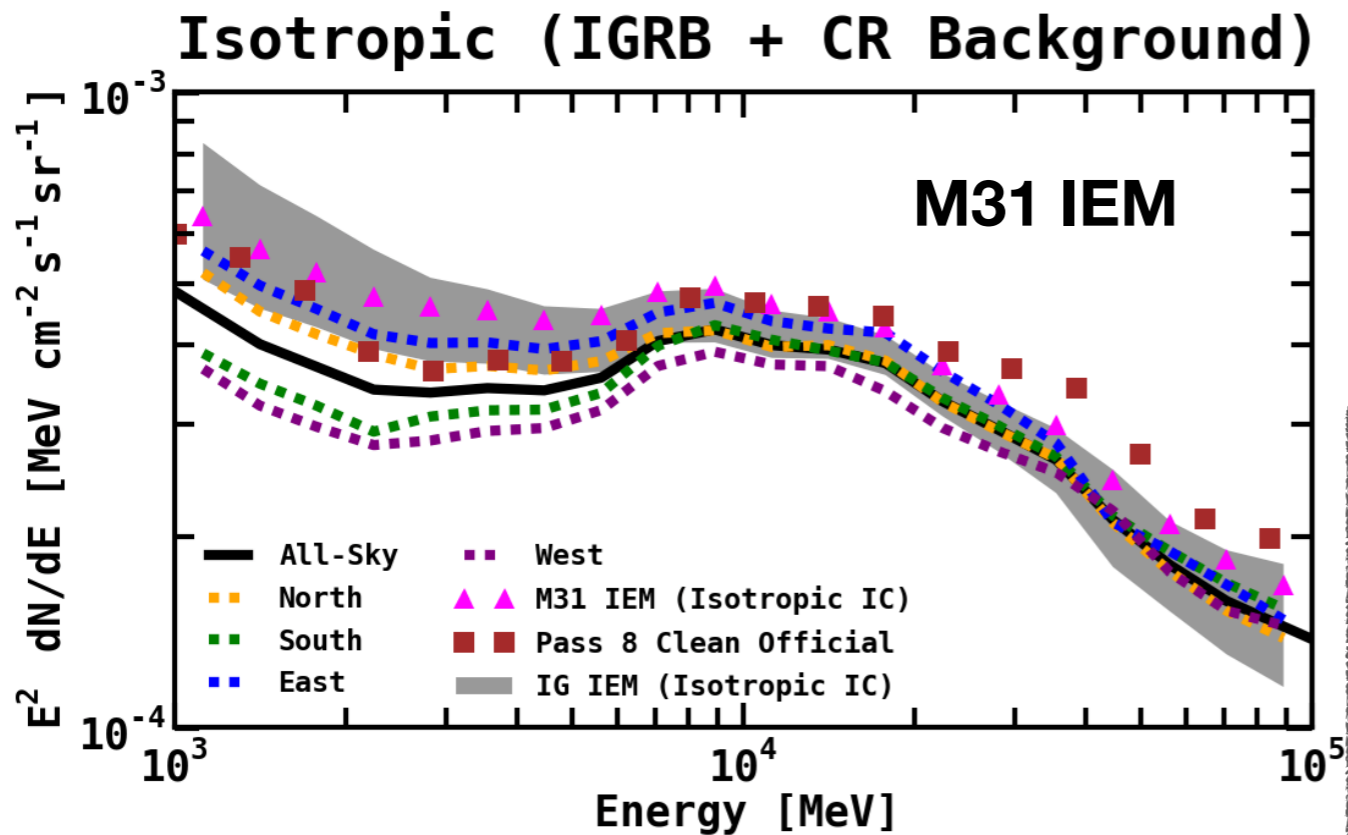


Table 2
Normalizations for Calculations of the Isotropic Component (M31 IEM)

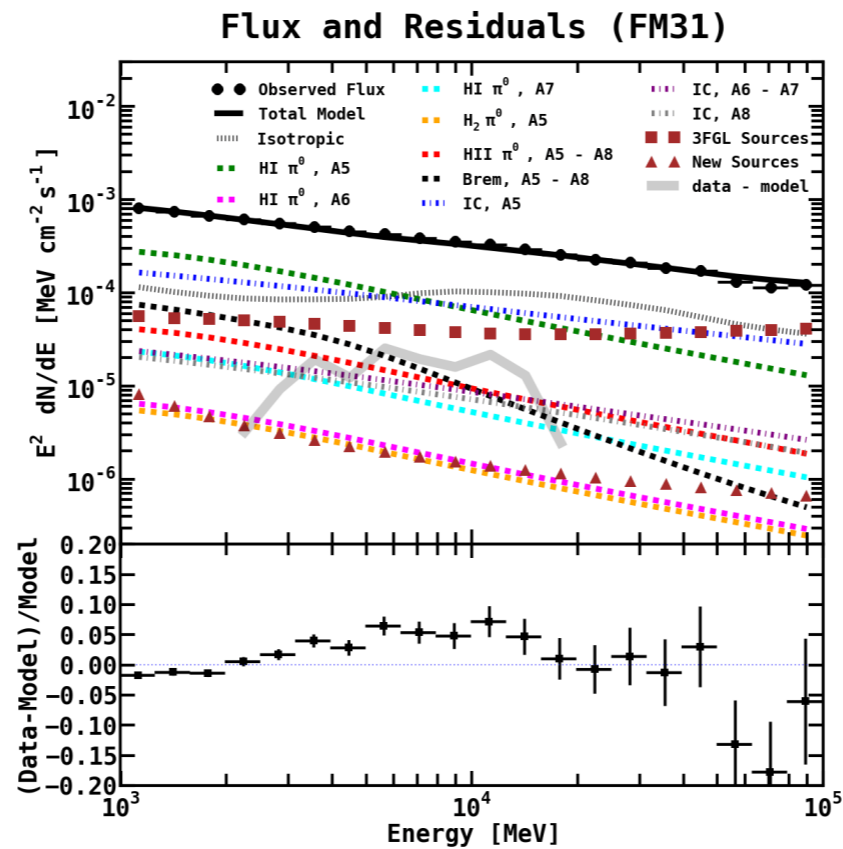
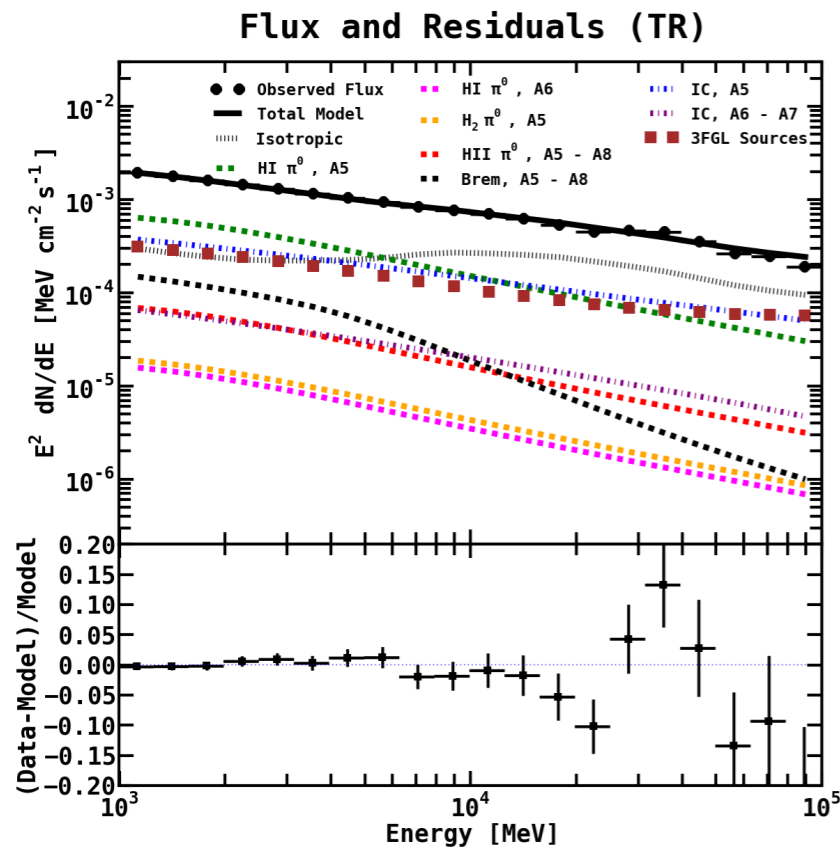
| Region | π^0 | AIC |
|---------|-------------------|-----------------|
| All-sky | 1.319 ± 0.005 | 1.55 ± 0.04 |
| North | 1.430 ± 0.010 | 1.14 ± 0.05 |
| South | 1.284 ± 0.006 | 1.86 ± 0.05 |
| East | 1.397 ± 0.009 | 1.07 ± 0.05 |
| West | 1.287 ± 0.006 | 1.88 ± 0.05 |

- We use the “all-sky” isotropic spectrum.
- Fit includes 3FGL sources fixed, sun and moon templates fixed, Wolleben component, all-sky π^0 decay and IC normalization scaled, and all-sky Bremsstrahlung fixed (see above table).
- Note that regardless of the fit variation, the spectrum of the isotropic contains a bump near ~ 10 GeV.

Systematic checks for the isotropic component:

- **The spectrum is calculated self-consistently with the M31 IEM.**
- **The normalization is determined in the TR: 1.06 ± 0.04 .** This remains fixed for all fits in FM31.
- **As a test, we freely scale the normalization of the isotropic component in FM31, along with the other sources.** The isotropic normalization obtains a value of 1.46 ± 0.06 . The residual emission remains qualitatively the same.
- **We repeat the analysis using the IG IEM, which has its own self-consistently derived isotropic component.** In this case the isotropic spectrum is determined at high latitudes, and the normalization remains fixed to its nominal value (1.0) for the fits in FM31.
- **We also repeat the analysis with the FSSC IEM and corresponding isotropic spectrum.** For this variation we use an extended energy range of 300 MeV - 300 GeV. The normalization of the isotropic component is fit in FM31 (along with the Galactic diffuse and point sources). The best-fit normalization is found to be 1.04 ± 0.005 .
- Using the FSSC IEM, **we repeat the analysis using both the Clean and UltraCleanVeto selection.**
- Although the residual emission in FM31 is found to be (very) roughly uniformly distributed over the entire field, **the residual emission in FM31 is not found to be isotropic.**

Results for Baseline Fit

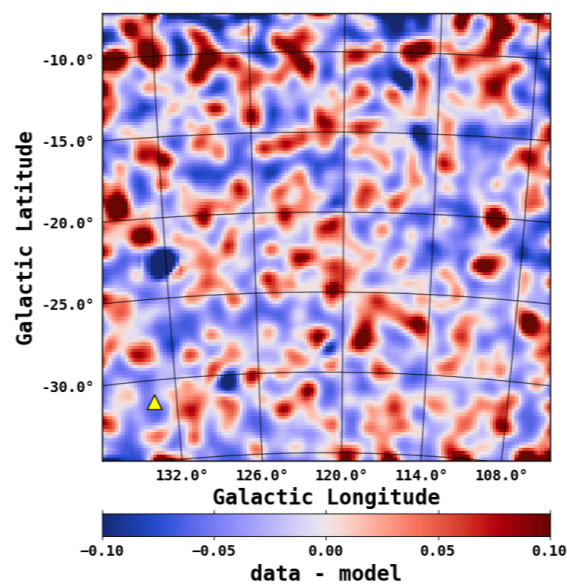
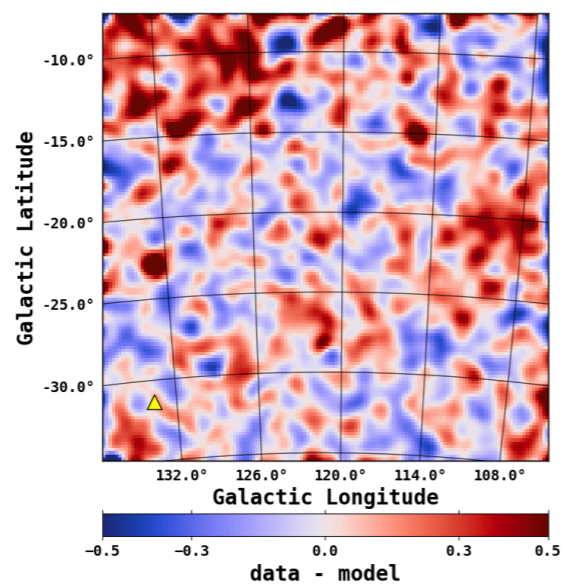
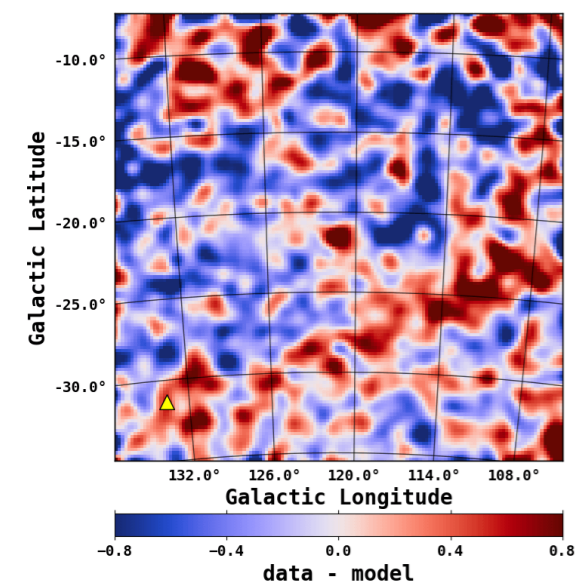


- Fit is performed by scaling the diffuse sources and point sources self-consistently.
- Flat residuals in the tuning region (TR).
- Positive residual emission in FM31 between ~ 3 -20 GeV at the level of $\sim 5\%$.
- Spatial residuals show structured excesses and deficits in the first energy bin—most notably, a large arc structure extending from the upper left corner around to the projected position of M33 (shown with a yellow triangle)
- The residual emission in the second energy bin (corresponding to the excess in the fractional count residuals) is more uniformly distributed, although the arc structure can still be seen.

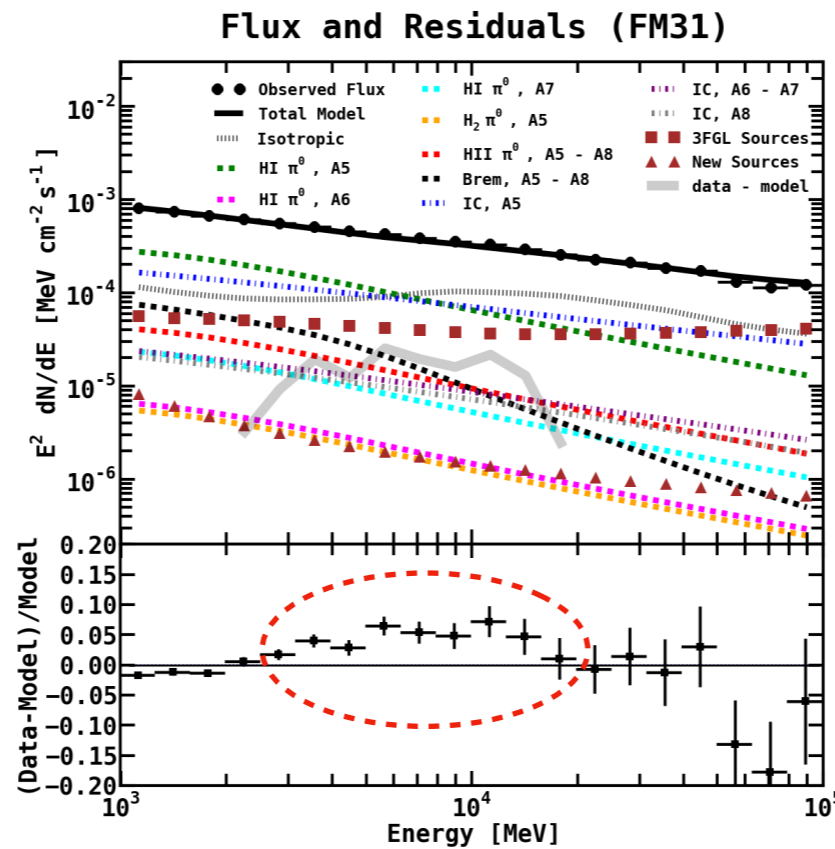
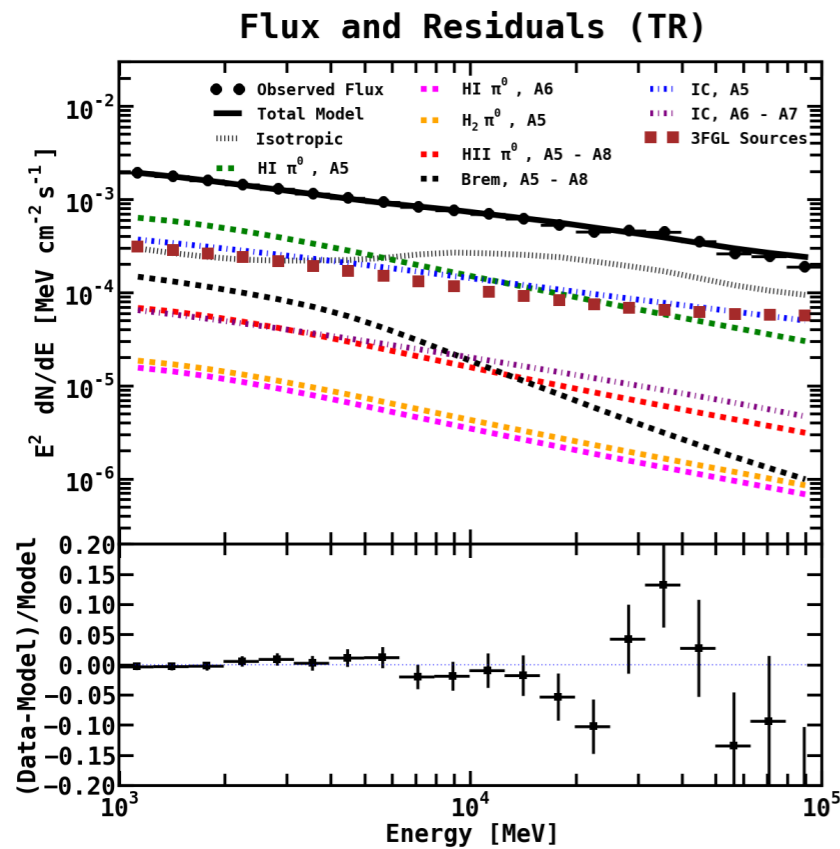
1 GeV - 3.2 GeV (FM31)

3.2 GeV - 20 GeV (FM31)

20 GeV - 100 GeV (FM31)



Results for Baseline Fit

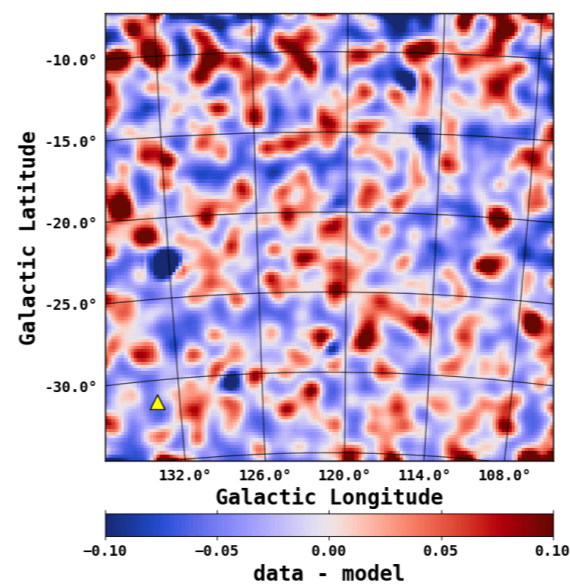
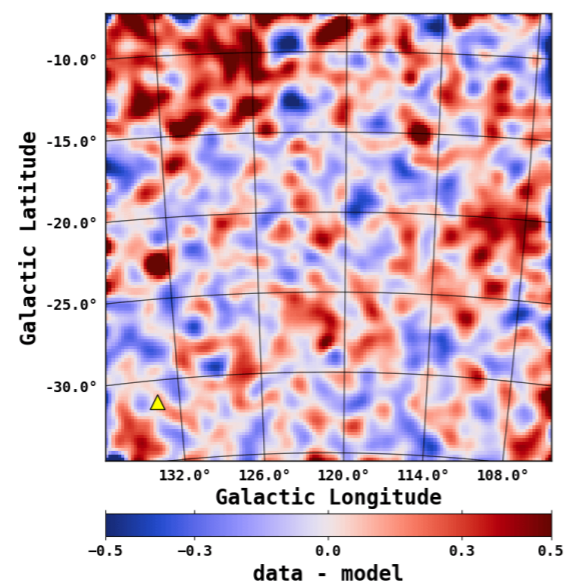
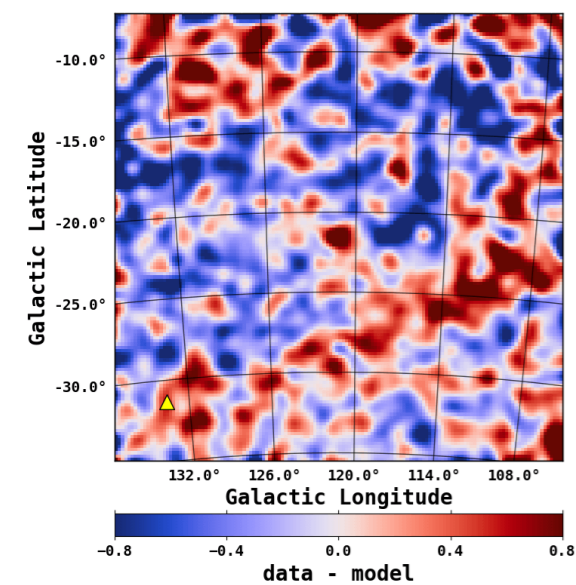


- Fit is performed by scaling the diffuse sources and point sources self-consistently.
- Flat residuals in the tuning region (TR).
- Positive residual emission in FM31 between ~ 3 -20 GeV at the level of $\sim 5\%$.
- Spatial residuals show structured excesses and deficits in the first energy bin—most notably, a large arc structure extending from the upper left corner around to the projected position of M33 (shown with a yellow triangle)
- The residual emission in the second energy bin (corresponding to the excess in the fractional count residuals) is more uniformly distributed, although the arc structure can still be seen.

1 GeV - 3.2 GeV (FM31)

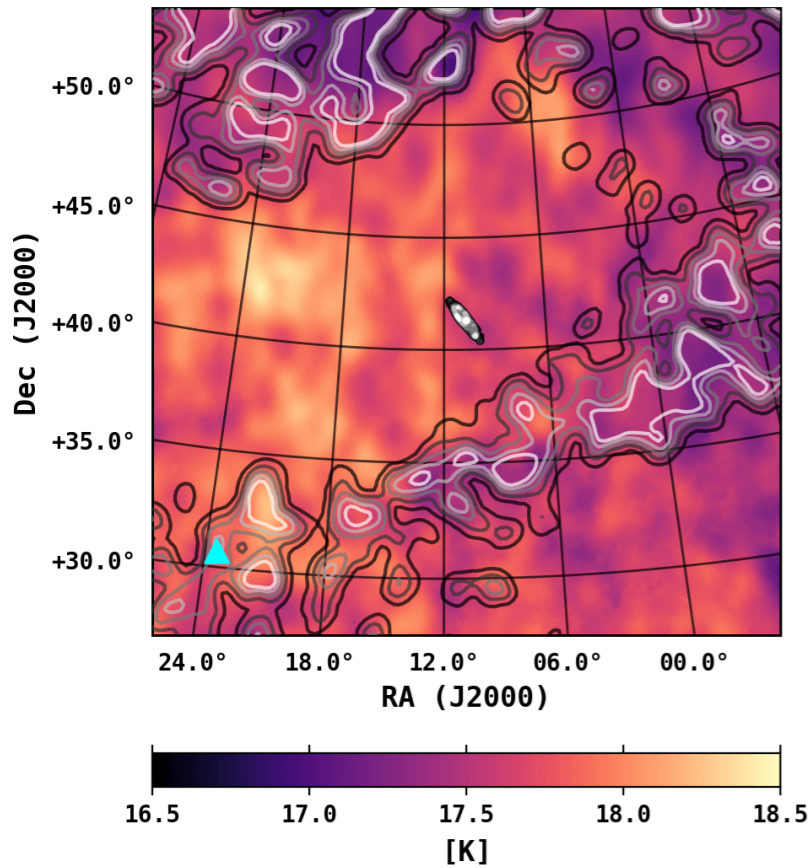
3.2 GeV - 20 GeV (FM31)

20 GeV - 100 GeV (FM31)

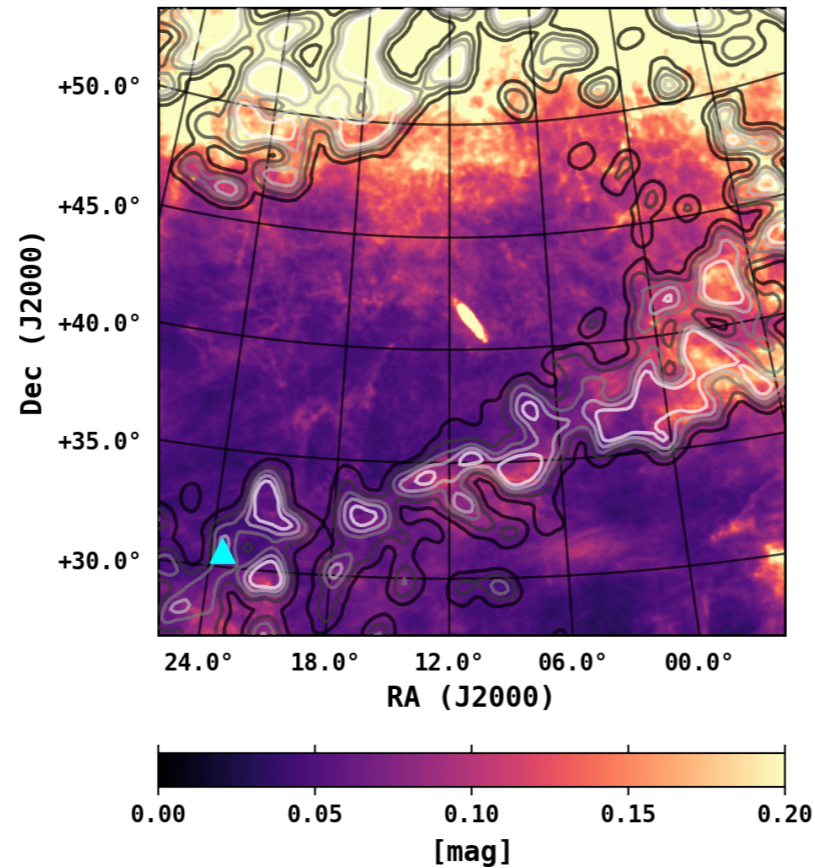


The Arc Template

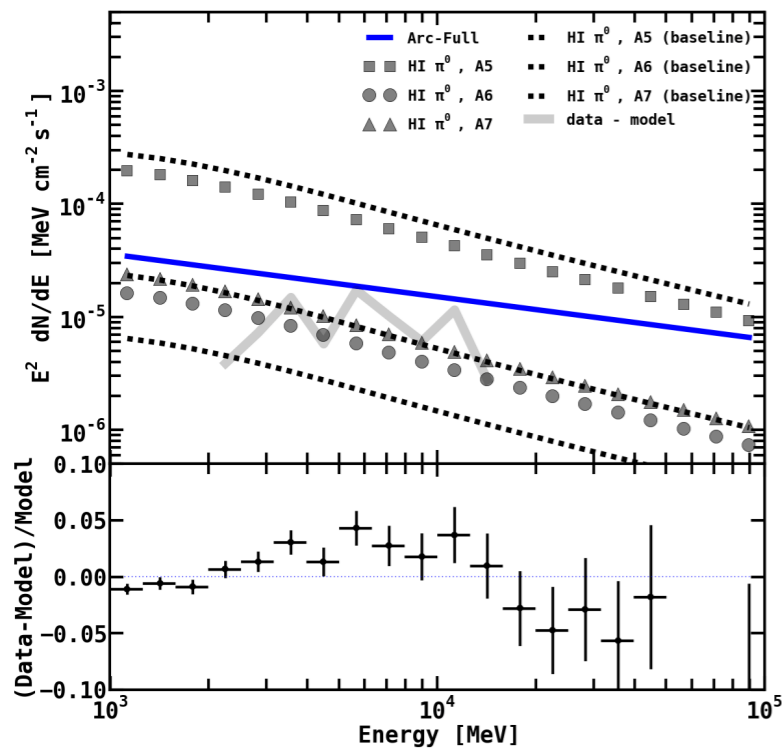
FM31 Dust Temperature



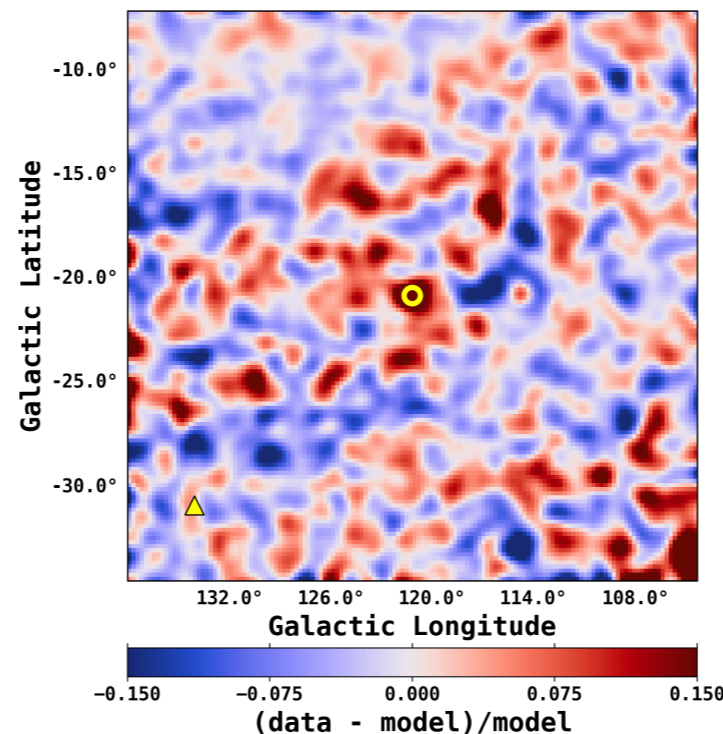
FM31 E(B-V) Reddening



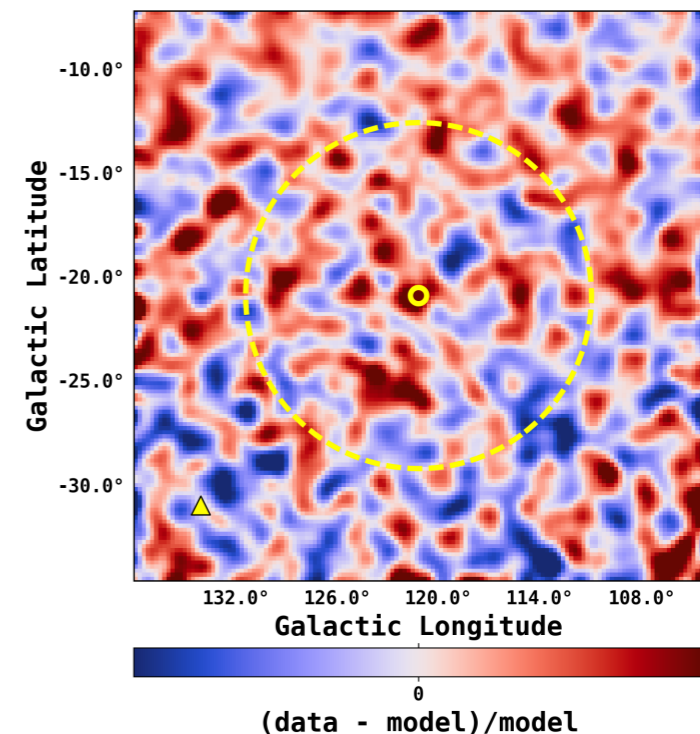
Arc Flux and Residuals



1 GeV - 3.2 GeV



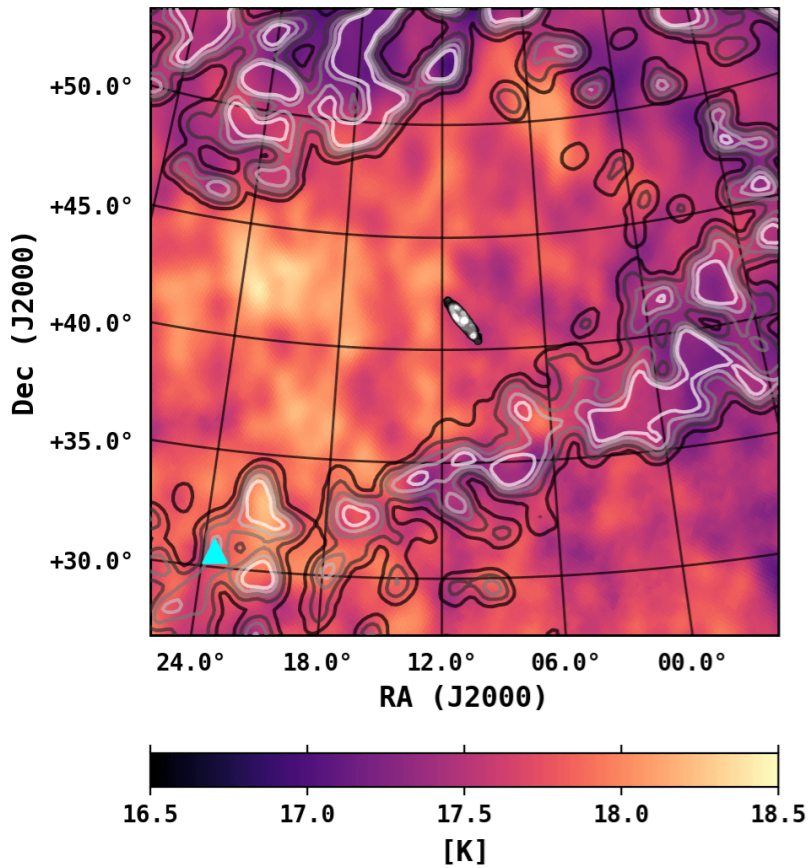
3.2 GeV - 20 GeV



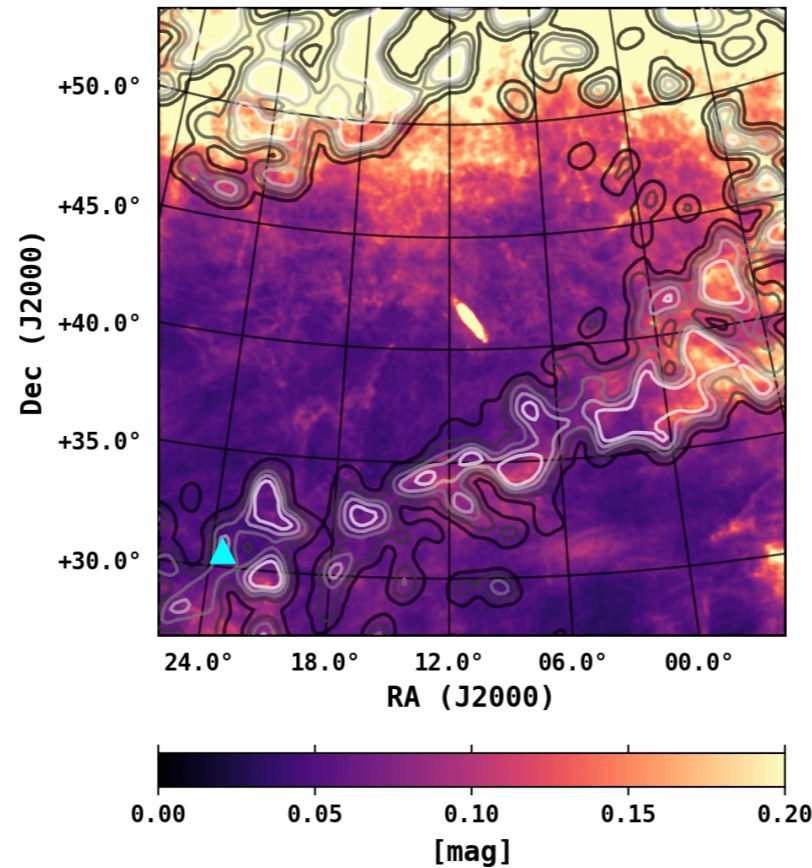
- Emission associated with the arc feature in the residuals is found to correlate with the local foreground HI column density, as well as properties of the dust, including regions where the dust is relatively cold.
- This may be an indication of a spatially varying spin temperature and/or inaccuracies in the modeling of the dark neutral medium (which is determined as part of an all-sky procedure).
- **We construct a template for the arc emission by selecting the positive residual emission in FM31 that correlates with tracers of the foreground gas and dust. We refer to this as the arc template.**
- Even with the addition of the arc template, the excess emission persists.

The Arc Template

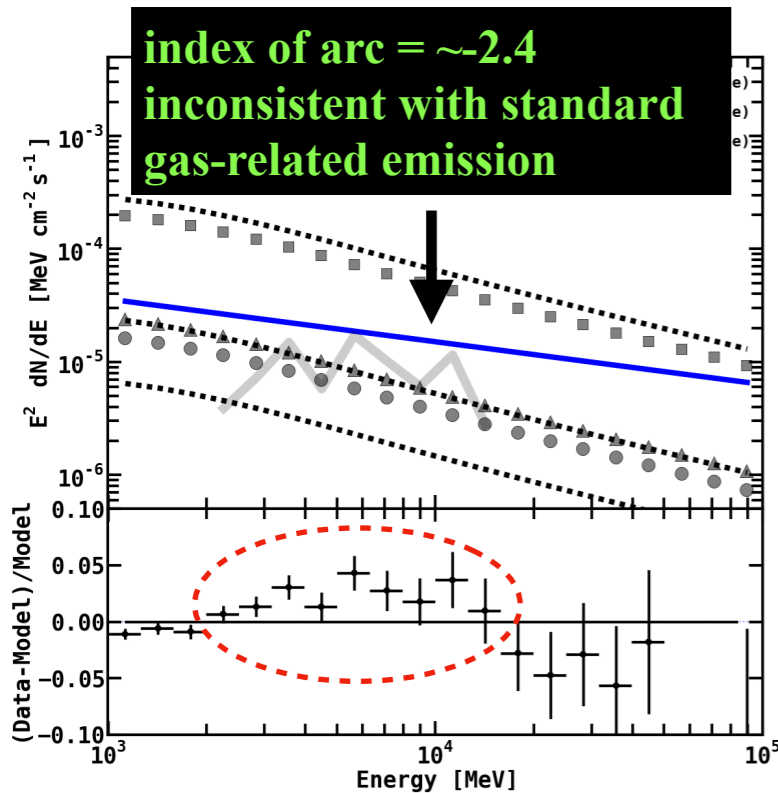
FM31 Dust Temperature



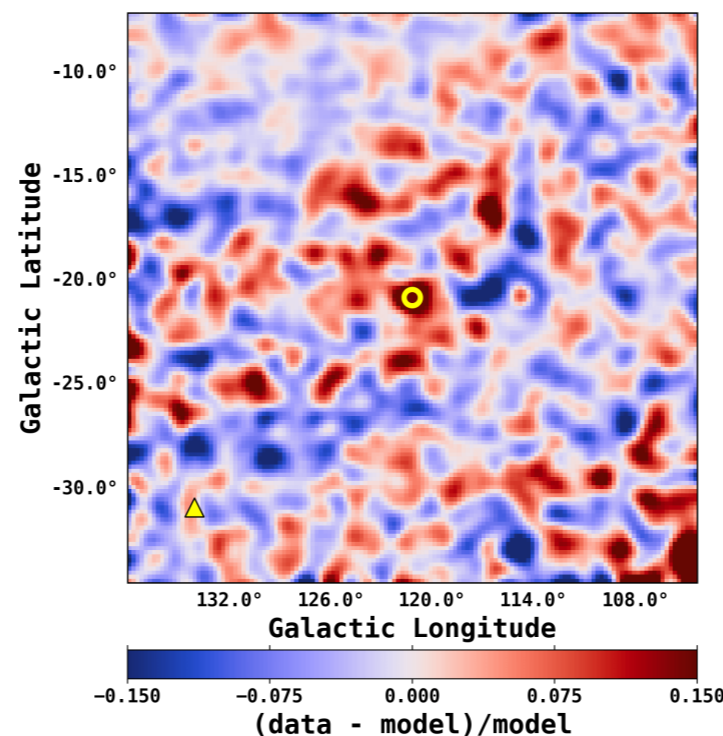
FM31 E(B-V) Reddening



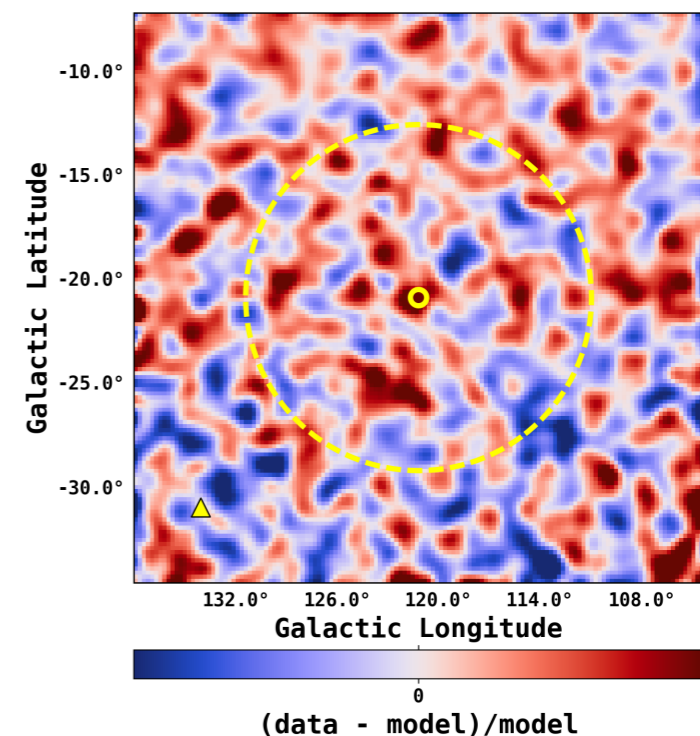
- Emission associated with the arc feature in the residuals is found to correlate with the local foreground HI column density, as well as properties of the dust, including regions where the dust is relatively cold.
- This may be an indication of a spatially varying spin temperature and/or inaccuracies in the modeling of the dark neutral medium (which is determined as part of an all-sky procedure).
- **We construct a template for the arc emission by selecting the positive residual emission in FM31 that correlates with tracers of the foreground gas and dust. We refer to this as the arc template.**
- Even with the addition of the arc template, the excess emission persists.



1 GeV - 3.2 GeV

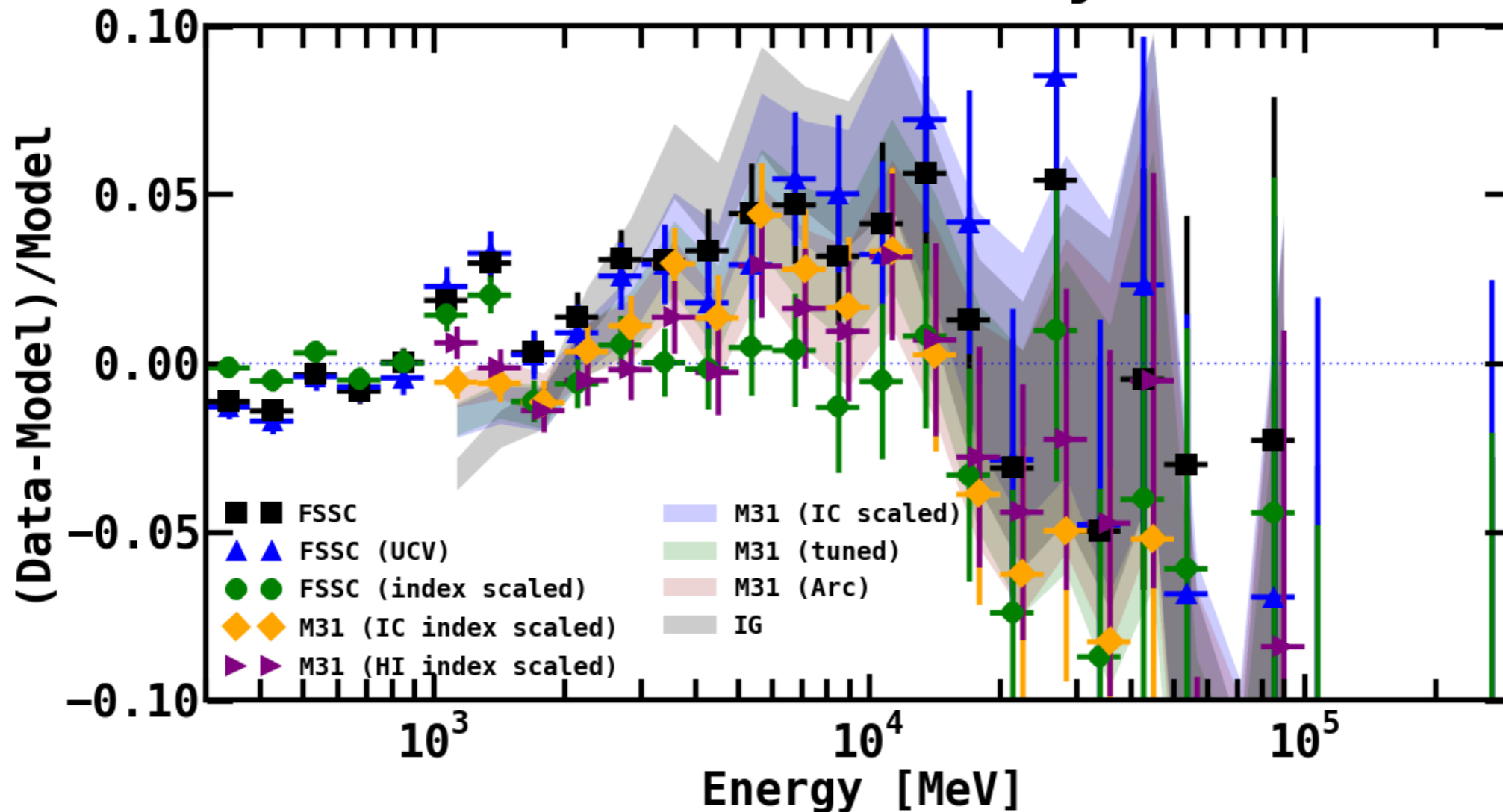


3.2 GeV - 20 GeV



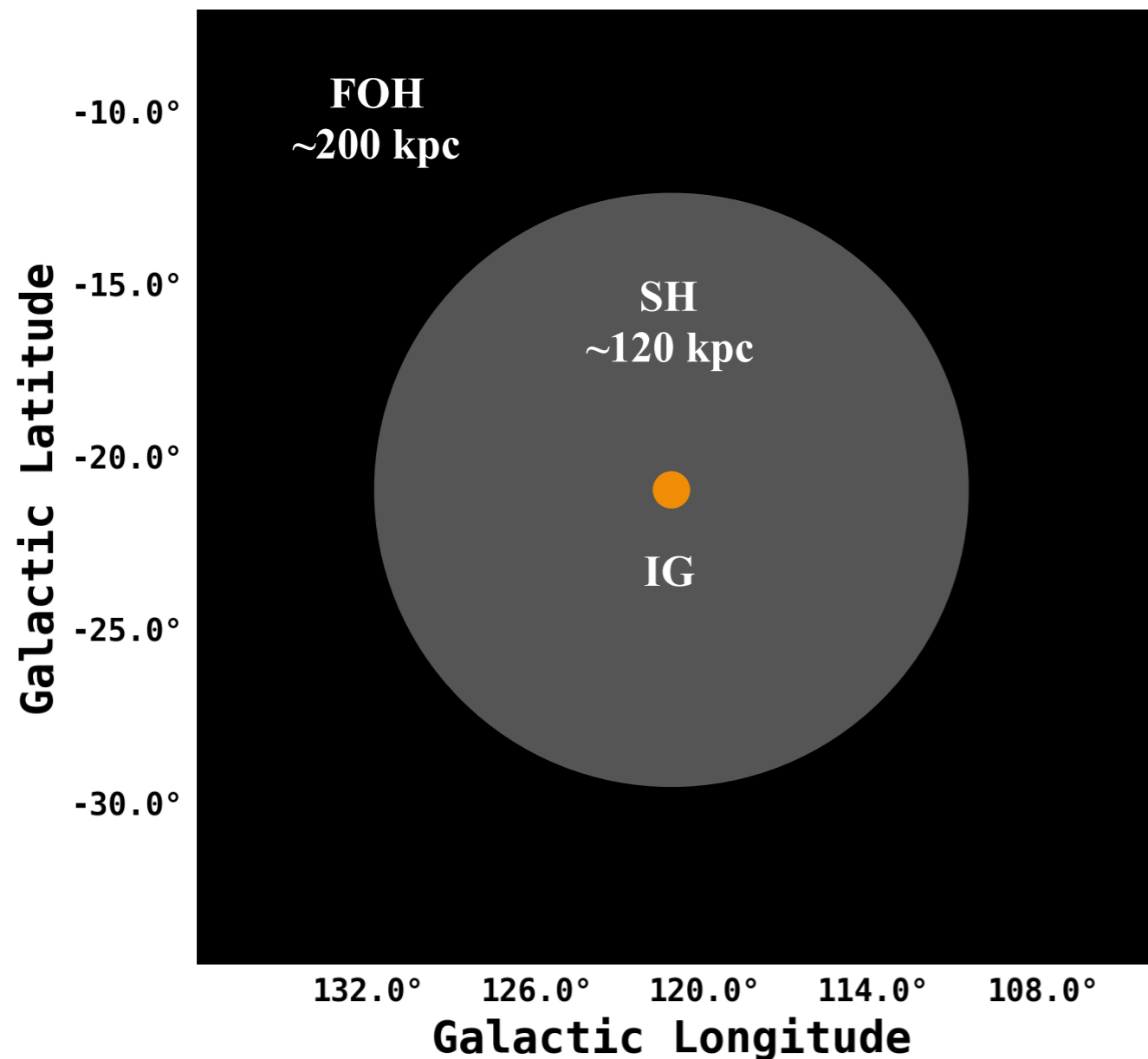
A Systematic Excess

Statistical (1σ) + Systematic



- We perform 9 main variations of the fit, using 3 different IEMs.
- We conclude that a systematic excess is present between ~ 3 -20 GeV at the level of ~ 3 -5%.
- The signal is only flattened with the FSSC IEM (intended for point source analysis), when fitting all components in the signal region (including the index of the Galactic diffuse component), whereas all other fits result in an excess. Our benchmark model is the M31 IEM.
- Our analysis shows that the characterization of the HI-related emission along the line of sight is a significant systematic uncertainty for observations towards M31's outer halo. All models we have tested use similar underlying HI maps. This will be fully addressed in a forthcoming work.

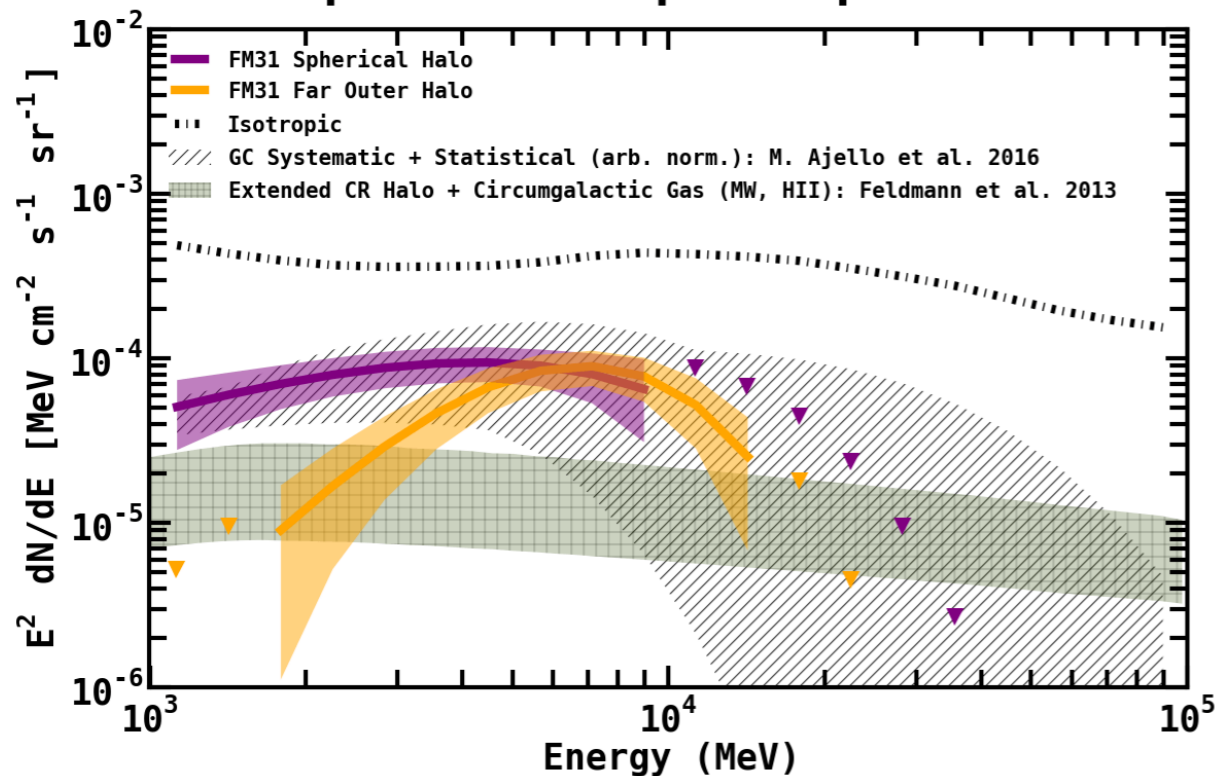
M31-Related Components



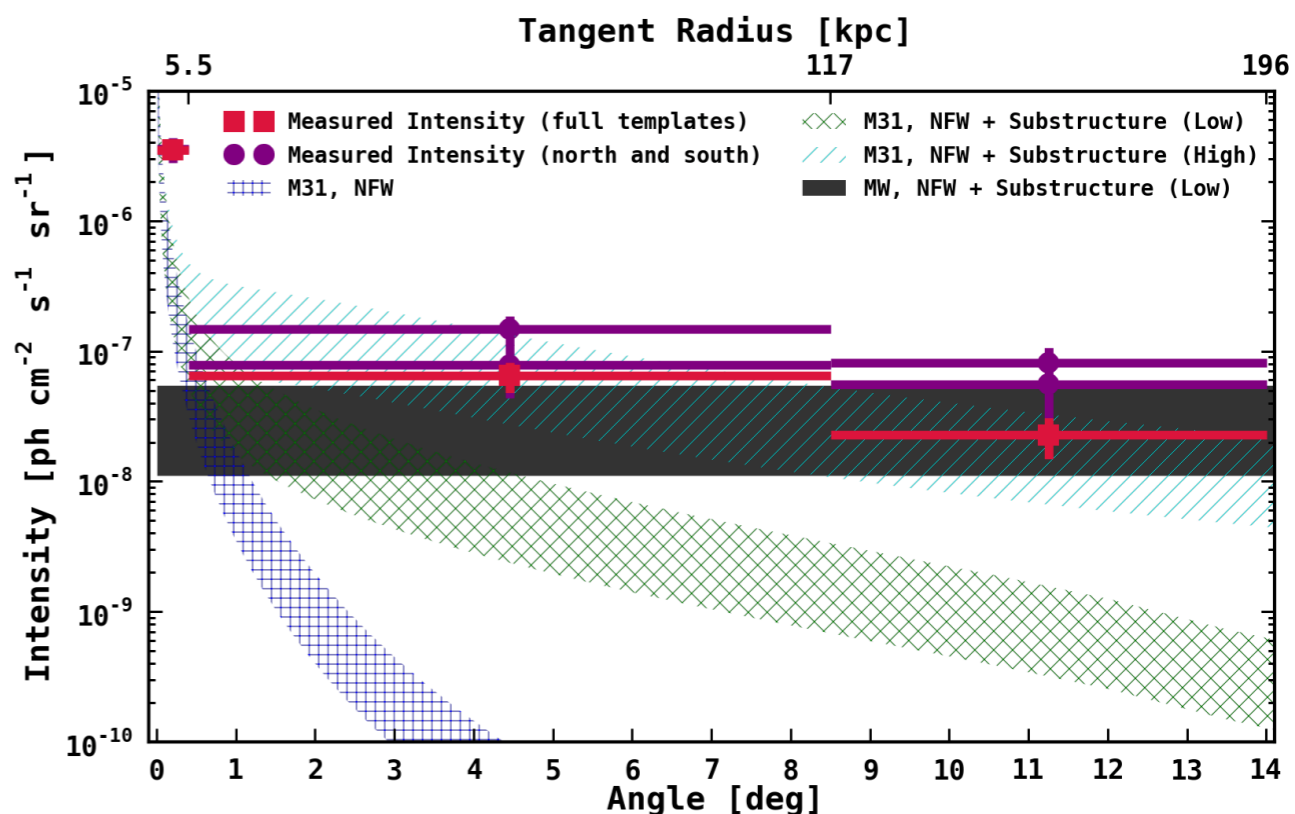
- Three components: inner galaxy (IG), spherical halo (SH), far outer halo (FOH).
- Fit components with PLEXP spectral model, self-consistently with other model components, including the arc template.
- IG consistent with previous detections
- SH and FOH significantly detected (>5 sigma)
- Addition of M31-related components flattens the excess in the fractional residuals

Results for M31-Related Components

Spectral Shape Comparison



FM31 Observed γ -ray Intensity



- Properties of M31's DM halo remain highly uncertain, i.e. geometry, extent, and substructure content. Likewise for the MW's DM halo.
- **We compare the observed excess with (simplified) predictions for a DM signal that originates from the M31 halo, with a spectrum and annihilation cross-section consistent with a DM interpretation of the GC excess.**
- We consider the contribution from both the M31 halo and the MW halo along the line of sight, since the MW component has not been explicitly accounted for in our analysis, and may be at least partially embedded within the isotropic component and other IEM components.
- We consider different assumptions for the amount of DM substructure in M31 (and the MW), and **we find that if a cold DM scenario is assumed that includes a large boost factor due to substructures, the observed excess emission is consistent with this interpretation.**
- Granted, however, the exact partitioning of individual contributions to the signal remains unclear, i.e. primary emission from M31's DM halo, secondary emission in M31, emission from the local DM filament between M31 and the MW, and emission from the MW's DM halo along the line of sight.

Summary and Conclusion

(arXiv:1903.10533)

- We present the first search for extended emission from M31 in gamma-rays out to a distance of ~ 200 kpc from its center.
- We perform an in-depth analysis of the systematic uncertainties related to the observations.
- We find evidence for an extended excess that appears to be distinct from the conventional MW foreground, having a total radial extension upwards of 120-200 kpc from the center of M31.
- The excess is found between ~ 3 -20 GeV at the level of ~ 3 -5%.
- We discuss plausible interpretations of the excess emission but emphasize that uncertainties in the MW foreground, and in particular, modeling of the H I-related components, have not been fully explored and may impact the results.
- The isotropic component is also an important systematic uncertainty when it comes to determining if the excess signal does in fact have a physical association with the M31 system.
- We find that a DM interpretation provides a good description of the excess emission and is consistent with the DM interpretation of the GC excess.
- We also find that the structured gamma-ray emission in FM31 is positionally coincident with numerous M31-related observations, and most notably, the M31 cloud (see paper).
- M31 is a very rich system, and more work is needed to better understand these new observations.

Thank You!